

Interactions and Reconnections of Four-Dimensional Quantum Vortices

H. A. J. Middleton-Spencer,^{1,*} B. McCanna,² D. Proment,³ and H. M. Price¹

¹*School of Physics and Astronomy, University of Birmingham, UK*

²*School of Computer Science, University of Birmingham, UK*

³*School of Engineering, Mathematics and Physics, University of East Anglia, UK*

(Dated: November 26, 2024)

Interactions and reconnections of vortices are fundamental in many areas of physics, including classical and quantum fluids where they are central to understanding phenomena such as turbulence. In three-dimensional (3D) superfluids, quantum vortices are one-dimensional (1D) filaments that can intersect, reconnect, and recoil with irreversible dynamics described by near-universal scaling laws. We explore quantum-vortex reconnections in a four-dimensional (4D) superfluid, where a vortex is a two-dimensional (2D) surface. Using real-time numerical simulations, we find much richer behaviour than in 3D, including stable intersecting vortex surfaces which do not reconnect, and unusual vortex reconnections which occur without significant energy dissipation, suggesting quasi-reversible dynamics. Our work raises many interesting questions about vortex physics in extra-dimensional systems, and may be extended in the future to more realistic experimental settings where the fourth dimension is simulated with techniques such as synthetic dimensions.

Vortex reconnections have long been of fundamental importance in many fields, ranging from plasma physics [1, 2] to classical [3–5] and quantum fluids [6–10]. These processes play a vital role in fluid dynamics as they provide a mechanism for the distribution of energy to multiple length scales throughout the system, and so underlie phenomena such as turbulence [3, 11–15], energy dissipation and relaxation towards equilibrium [16–18].

In quantum fluids, vortex reconnections have been observed experimentally both in liquid Helium [6, 7] and in Bose-Einstein condensates (BECs) [8]. Unlike the arbitrary circulation and size allowed in classical fluids, quantum vortices are characterised by a quantized circulation around a fixed-size “vortex core” of vanishing superfluid density [19–29]. In 3D, a quantum vortex has a core described by a 1D tube or “filament”, corresponding to a topological defect in the order parameter. Vortex reconnections are then dramatic events, occurring at a specific time, t_0 , when the core topology changes [10, 30–32]. Physically this corresponds to, for example, two vortex filaments intersecting and exchanging tails, before moving apart.

Remarkably, the dynamics of 3D vortex reconnections is universal at small scales [33], with the minimum distance between the vortex lines, δ , varying near the reconnection as

$$\delta(t) \approx \mathcal{A}^\pm (\kappa |t - t_0|)^{1/2}, \quad (1)$$

where $\kappa = h/m$ is the quantum of circulation, with Planck’s constant h and particle mass m , and where \mathcal{A}^- (\mathcal{A}^+) is a dimensionless scaling parameter before (after) the reconnection time, t_0 [10, 34, 35]. Generically, $\mathcal{A}^+ > \mathcal{A}^-$, reflecting that vortices repel faster than they approach [17, 34, 36, 37]; this is linked to the transfer of energy from the vortex core into sound and Kelvin waves [17, 37, 38] as well as a loss of vortex-core length, meaning that 3D vortex reconnections are statistically

irreversible.

In this Letter, we investigate vortex interactions and reconnections in a superfluid with *four spatial dimensions*. This builds on recent work studying how, in a 4D BEC, a quantum vortex takes the form of 2D planes [39], or more generally surfaces [40, 41]. As we now show with real-time dynamical simulations, the resulting 4D quantum vortex reconnections are much richer than their 3D counterpart, with very different dynamics being observed depending on the initial reconnecting surface. We focus on three classes of configurations for which we observe, respectively, no reconnections; 3D-like reconnections accompanied by the transfer of energy into sound waves; and unusual 4D reconnections, in which there is no appreciable energy transfer, suggesting the dynamics may be quasi-reversible in a statistical sense. Unlike for extended vortex lines in 3D, the vortex in each case remains a single connected surface throughout the real-time dynamics, even as the topology of this surface changes through reconnection. This behaviour can occur in 3D, but only when a compact vortex ring reconnects with itself.

Our work paves the way for future studies of vortex reconnections, vortex dynamics, and turbulence in higher spatial dimensions. This is not only of fundamental interest, but is motivated by experimental advances in simulating 4D physics, e.g. with approaches such as synthetic dimensions [42–66], using which 4D atomic systems have recently been experimentally realized [67, 68]. While here we have studied a minimal model for a 4D BEC, in the future, it will also therefore be interesting to explore vortex reconnections in these more realistic experimental systems [69] and draw connections with other higher-dimensional mathematical models describing high-energy/string theory physical systems [70, 71].

4D Quantum Vortices: We model our system as a bosonic quantum fluid in the zero-temperature mean-

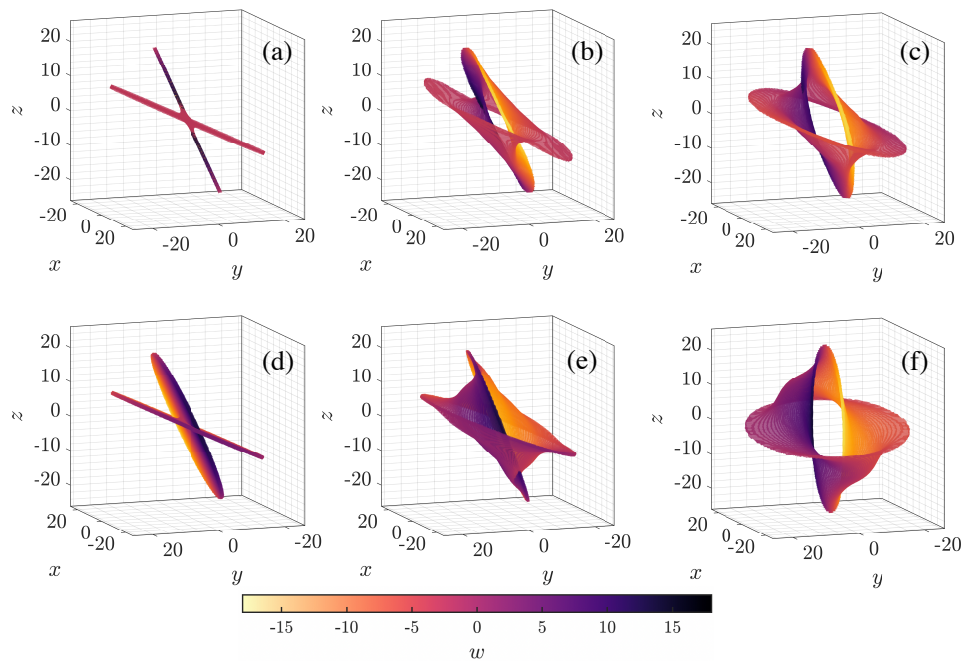


FIG. 1. Numerical real-time dynamics of the 4D GPE for an input wave function containing two vortices intersecting at the origin [c.f. Eq. (6)]. (*Top Row:*) The input state has $\theta_1 = 50^\circ$, $\theta_2 = 0$ [c.f. Eq. (4)], corresponding to planar-aligned vortices, shown for (a) $t = 0$, (b) $t = 50$, (c) $t = 100$, which is classified as a 4D generalisation of 3D reconnection. (*Bottom Row:*) The input state has $\theta_1 = -\theta_2 = 50^\circ$, corresponding to anti-aligned vortices, shown for (d) $t = 0$, (e) $t = 50$, (f) $t = 100$, which is a new type of reconnection not observed in 3D systems. In both cases the vortices reconnect, opening up a hole around the origin which grows in time. The figures are presented in the (x, y, z) subspace, with w denoted by colour.

field limit, where the condensate is described by a single order parameter wave function, ψ . The dynamics of ψ are governed by the dimensionless 4D Gross-Pitaevskii equation (GPE) [39–41]

$$i \frac{\partial \psi'(\mathbf{x}', t')}{\partial t'} = \left[-\frac{1}{2} \nabla'^2 + V(\mathbf{x}') + |\psi'(\mathbf{x}', t')|^2 \right] \psi'(\mathbf{x}', t'), \quad (2)$$

where $\mathbf{x}' = (x', y', z', w')$, denoting the four Cartesian dimensions. Equation (2) has been rescaled into natural units: $\mathbf{x}' = \mathbf{x}/\xi$, (where ξ defines the healing length of the system), $t' = t/\tau$, (where $\tau = \hbar/\mu$), and $\psi' = \psi/\sqrt{\mu/g}$, where μ and g are the chemical potential and interaction strength of the system. For brevity, primes will now be dropped.

Similar to 2D and 3D, the 4D GPE supports quantum vortex solutions; in the simplest case, a 4D vortex is described by a wave function of the form $\psi_1(\mathbf{x}) = f_k(r_1)e^{ik\phi_1}$, where (r_1, ϕ_1) are the polar coordinates defined within a given 2D plane (e.g. the x - y plane); the wave function's magnitude, $|\psi_1(\mathbf{x})| = f_k(r_1)$, is a real-valued function which vanishes as $r_1 \rightarrow 0$, corresponding to a vortex spanning the entire orthogonal 2D plane (e.g. the z - w plane). As in lower dimensions, the phase of the field then winds around the vortex an integer k number of times, inducing an in-plane superfluid velocity field $\mathbf{v}_1 = k\hat{\phi}_1/r_1$.

Hereafter we focus on the case $k = 1$, which can be en-

ergetically stabilised by rotating the 4D superfluid with respect to the given 2D plane [39] and we are interested in how two such vortices dynamically reconnect within a 4D superfluid. We define a reconnection of superfluid vortices in arbitrary dimensions as a point in time where the topology of the vortices changes. This is the standard definition used in 3D both for superfluids [30–32], and – originally – for classical fluids where tubes of vorticity replace quantized vortices [72]. More precisely, let $\mathcal{C}(t) = \{\mathbf{x} \in D \mid \psi(\mathbf{x}, t) = 0\}$ be the set of vortices at time t , where $D \subset \mathbb{R}^d$ is the region containing the superfluid (excluding its boundary): a reconnection then occurs at a time $t = t^*$ if and only if $\mathcal{C}(t^*)$ is not homeomorphic to $\mathcal{C}(t)$ for times either immediately before t^* or immediately after (or both) [see Supplementary Material (SM) for a discussion of this definition]. Note that this definition assumes that ψ can only vanish on the boundary of the superfluid or on a vortex. This is not true in general, but it applies in all of our numerical simulations.

Similar to in lower dimensions, the dominant contribution to the interaction energy between two vortex planes in a large, homogeneous system is given by the hydrodynamic kinetic energy, $E_h \approx \int \frac{\rho}{2} \mathbf{v}^2 d^4r$ where $\rho = |\psi|^2$ is the density, and $\mathbf{v} = \mathbf{v}_1 + \mathbf{v}_2$ is the total velocity field found by summing the velocities of the individual vortices [40]. This can therefore be decomposed into a sum of the energies of each individual vortex along with the

hydrodynamic vortex-vortex interaction energy [40]

$$E_{vv} \approx \int \rho \mathbf{v}_1 \cdot \mathbf{v}_2 d^4r, \quad (3)$$

which can be positive (i.e. repulsive) or negative (i.e. attractive), depending on the relative orientation of the two vortex planes.

We will parametrise these non-orthogonal vortex plane states symmetrically as follows: given \mathbf{x} the spatial coordinates in the lab frame, we define two new frames \pm , with respective coordinates \mathbf{x}^\pm . These are defined in relation to each vortex plane and are each tilted from the lab frame in an equal and opposite way to each other. That is, these vortex frames are related to the lab frame by $\mathbf{x}^\pm = R(\pm\theta_1/2, \pm\theta_2/2)\mathbf{x}$, and therefore to each other by $\mathbf{x}^+ = R(\theta_1, \theta_2)\mathbf{x}^-$, where $R(\theta_1, \theta_2)$ is a double rotation which we can assume without loss of generality to take the form [40]

$$R(\theta_1, \theta_2) = \begin{pmatrix} \cos \theta_1 & 0 & -\sin \theta_1 & 0 \\ 0 & \cos \theta_2 & 0 & -\sin \theta_2 \\ \sin \theta_1 & 0 & \cos \theta_1 & 0 \\ 0 & \sin \theta_2 & 0 & \cos \theta_2 \end{pmatrix}, \quad (4)$$

where $\theta_{1,2} \in (-\pi/2, \pi/2)$. We then have that one vortex lies in the $z^- - w^-$ plane (inducing rotation in the $x^- - y^-$ plane as described above), while the other lies in the $x^+ - y^+$ plane (inducing rotation in the $z^+ - w^+$ plane). The two angles θ_1 and θ_2 therefore define the relative initial orientation of the two vortices, which intersect at the origin. Note that the simplest case, $\theta_1 = \theta_2 = 0$, corresponds to having two completely orthogonal intersecting vortex planes; in this case, E_{vv} vanishes as the resulting velocity fields are also orthogonal. Unlike in lower dimensions, this intersecting vortex configuration can be energetically stabilised by a suitable ‘‘double rotation’’ of the superfluid [39] with two equal frequencies. More generally, if $\theta_1 = \theta_2$ then the two vortices are in an aligning configuration and can be energetically stabilised by a double rotation with generically unequal frequencies [40].

In this Letter, we will focus on the dynamics associated with three classes of configurations: the (1) *aligning* case, when $\theta_1 = \theta_2$, where the two vortices hydrodynamically repel each other, (2) the *planar-aligning* case, when $\theta_2 = 0$ and $\theta_1 > 0$, where the hydrodynamic interaction energy vanishes by symmetry, and (3) an *anti-aligning* case, when $\theta_1 = -\theta_2$, where vortices hydrodynamically attract each other [40]. All the following angles are therefore expressed in terms of θ , where $\theta \equiv \theta_1$.

For short times t and small distances (i.e., $t, x < 1$) from the reconnection point we can analytically examine the dynamics using the linearised GPE model (i.e. the Schrödinger equation). This predicts that the evolution of the non-orthogonal planes is approximated by [41]

$$\psi = i(\sin \theta_1 - \sin \theta_2)t + (x^- + iy^-)(z^+ + iw^+). \quad (5)$$

In particular, this predicts that aligning planes ($\theta_1 = \theta_2$) do not reconnect – and in fact form a stationary state – which remains to be seen in the full nonlinear dynamics. In the general $\theta_1 \neq \theta_2$ case the linearized dynamics predict a reconnection that always consists of a hole opening in the vortex surface [41]. For that reason we only look at the special cases of aligning, planar-aligning, and anti-aligning tilt in this Letter.

Numerical Simulations: We solve the 4D GPE (2) using a fourth-order Runge-Kutta scheme for time evolution and standard finite-difference methods for computing spatial derivatives. The spatial domain is discretised by a uniform step $dx = 0.5$ in each direction, which ensures that the vortex core ($\sim 5\xi$) is well sampled numerically, and the time step is set to $dt = 0.025$. In all simulations, we include a hard-wall hyper-spherical potential with $V(\mathbf{x}) = 10$ if $r^2 \geq R^2$, and which vanishes otherwise, where $r = \sqrt{x^2 + y^2 + z^2 + w^2}$ and $R = 30$ being the radius of the boundary. The wave function at $t=0$ is given by

$$\psi(\mathbf{x}) = \psi_0(\mathbf{x})F(r_1^-)e^{i\phi_1^-}F(r_2^+)e^{i\phi_2^+} \quad (6)$$

where ψ_0 is the numerical solution for the ground state in the external potential with no vortices, (r_1^-, ϕ_1^-) and (r_2^+, ϕ_2^+) are polar coordinates in the $x^- - y^-$ and $z^+ - w^+$ planes, respectively, and $F(r)$ is the radial function given by the Padé approximation [73] of a vortex core on a uniform background. The results are ran briefly in imaginary time, before being run in real time to study dynamics. Note that visualisation of 4D vortices has obvious difficulties; we choose to depict the vortex surfaces in the (x, y, z) subspace, with the w direction denoted by the colour of the image, see e.g. Fig 1.

Aligning Vortices: When $\theta_1 = \theta_2 = \theta$, the vortices are initially in an aligning orientation. For example, as $\theta \rightarrow \pi/2$, we see from Eq. 4 that $x^- + iy^-$ and $z^+ + iw^+$ approach each other, meaning that the two vortices overlap in the same plane. More generally, for aligning vortices, it can be shown that Eq. 3 becomes $E_{vv} = -4\mu N \frac{\xi^2}{R^2} \ln(\cos \theta)$, where μ is the chemical potential and N is the number of particles, corresponding to a positive interaction energy [40]. Interestingly, we find that, despite this repulsive vortex-vortex interaction, aligned vortices do not reconnect in the real-time dynamics, but instead continue to intersect at the origin while rotating around each other freely, akin to the Abrikosov lattice in two- and three-dimensional systems [28, 74]. The lack of reconnection is consistent with previous results for a simple linear expansion of the short-term dynamics near the vortices [41]. Similar stationary states with intersecting vortex lines have also been found in 3D [75] (the simplest being two intersecting, orthogonal lines), although these require more symmetry than our aligning states, and cannot be energetically stabilised by rotation, unlike non-orthogonal vortex planes in 4D [40].

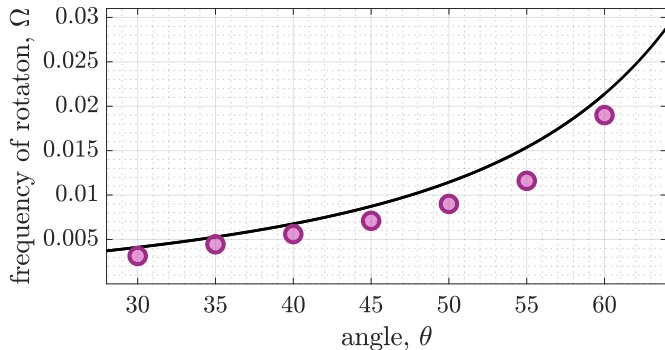


FIG. 2. The frequency of precession in the $x-w$ plane, Ω_{xw} , of two aligning vortices for each aligning angle, θ , in a smaller system of radius $R = 18$. The analytical solution (*black line*) from Eq. (7) is compared to the frequency of the rotation measured computationally (*purple*).

As derived in the Supplemental Material, the frequency, Ω , of the rotation is given by,

$$\Omega = \frac{2 \tan \theta}{R^2 \cos \theta}, \quad (7)$$

and agrees with the computational results (Fig. 2).

Planar-aligning Vortices: In this case, we have that $\theta_1 = \theta > 0$ and $\theta_2 = 0$, corresponding to the x^- and z^+ axes being tilted towards each other, while $y^- = y$ and $w^+ = w$ are unaffected. In this special case, the hydrodynamic interaction between the vortices vanishes by symmetry, regardless of the value of θ [40]. When $\theta \rightarrow \pi/2$, both x^- and z^+ approach $(x+z)/\sqrt{2}$, such that the two vortices intersect along the line given by $x = -z$, $y = w = 0$. In any 3D cross-section of the system orthogonal to this line the vortices will appear as two intersecting lines. We can therefore expect this limit to give a 4D generalisation of the usual 3D vortex reconnection physics [10].

Numerically, we find that in our real-time dynamics, two planar-aligning vortices will indeed reconnect, causing a hole to open up at the intersection point around the origin, as shown in Fig. 1(a,b,c) for $\theta = 50^\circ$. It can also be shown analytically that the reconnected core is homeomorphic to a punctured plane (see Supplemental Material). Unlike for extended vortex lines in 3D, the vortex remains a single connected object throughout the real-time dynamics. Instabilities along the vortex surface also form during the reconnection, shown as small density ripples along the vortex at large post-reconnection times.

To quantify the reconnection dynamics, we describe the hole around the origin as an ellipse and extract the semi-minor axis as a measure of the minimum distance between the vortices arising from the reconnection. This approximation is found to give a precise description of the size of the reconnection region and is similar to considering the minimum distance between two vortex lines after

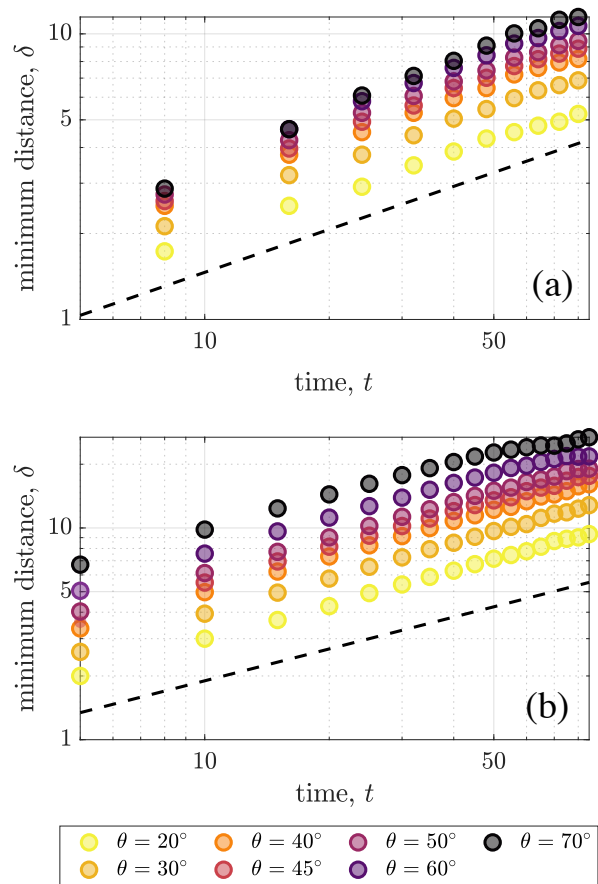


FIG. 3. The change in the minimum distance, δ , between vortices (as defined in the main text) within the reconnection zone as obtained from the real-time dynamics [c.f. Fig 1] for (a) initially planar aligned vortices and (b) initially anti-aligned vortices. Both orientations show a post-reconnection scaling law, $\delta(t) \sim t^{1/2}$, matching the 3D result in Eq. (1). The scaling $t^{1/2}$ (*dashed*) is marked for reference.

they reconnect in 3D [7, 33, 34, 36, 37, 76]. By measuring this minimum distance within the reconnected region over time, we find that the same universal scaling law in Eq. (1) also holds for reconnection of two planar-aligning vortices in four dimensions, as can be seen in Fig. 3(a). This aforementioned scaling corresponds to $\sim t^{1/2}$ (Eq. 1), which is plotted for reference in Fig. 3(a), and verifies that the scaling is observed in the planar reconnection case, for all reconnection angles θ . As in 3D, we observe that this reconnection process is irreversible, with the energy associated with the vortex core - i.e. the *incompressible energy*, E_i - being transferred into sound energy. There is also formation of Kelvin waves along the vortex plane. This energetic transfer is shown in Fig. 4(a), where we observe a clear downwards trend in the incompressible energy over time, becoming more marked with increasing values of θ as the initial vortex configuration tends towards the 3D-like limit. Note that the

typical way of calculating the incompressible energy is through a Helmholtz decomposition; however, this is not valid in a 4D system, and thus a generalised Helmholtz decomposition must be used instead, as detailed in the Supplemental Material. We have therefore shown that the reconnection of two planar vortices in a 4D condensate follows all of the generalised laws observed in the reconnection of vortices in a 3D condensate.

Anti-aligning Vortices: We lastly study the case with $\theta = \theta_1 = -\theta_2$. Then as $\theta \rightarrow \pi/2$, we have that $x^- + iy^-$ and $z^+ + iw^+$ becomes complex conjugates of each other, meaning that the two vortices anti-align within the same plane (and would potentially annihilate). More generally, it can be shown that the hydrodynamic vortex-vortex interaction energy has the same form as stated for the aligning case above, except with the opposite sign, corresponding to a negative interaction energy [40].

Numerically, our real-time dynamical simulations find that two anti-aligned vortices will reconnect around the origin, as shown in Fig. 3(b) for $\theta = 50^\circ$. This is similar to the planar-aligning case and is also consistent with a previous prediction from a simple linear argument for the short-time dynamics near the vortices [41], like in the aligning case. We can also again quantitatively characterise the 4D reconnection dynamics by plotting the minimum distance obtained from the semi-minor axis of the reconnection zone in Fig. 3(b). We again see a clear $t^{1/2}$ scaling, in agreement with the scaling of both 3D reconnection dynamics and the 4D planar-aligned case discussed above, with a small flattening out at the late times due to finite size effects. However, an interesting and immediate difference here is the lack of fluctuations of the vortex planes. The incompressible energy also does not significantly vary on average over time, as shown in Fig. 4 (b), suggesting that the reconnection may be reversible.

Conclusions: With the plethora of recent works on extra-dimensional physics in cold atomic systems, this work provides the first systematic study of vortex dynamics in a condensate with an extra physical dimension. The study of vortex formation has often been a first aim for any experimentalist studying a new form of quantum fluid; it is thus hoped that with the fast moving field of synthetic dimensional physics that vortices can be observed soon in a four dimensional condensate.

We have characterised three different ways that quantum vortices can interact and reconnect in a 4D superfluid, going beyond the physics of lower-dimensional systems. Firstly, when the two vortices are in an aligning orientation, there is no reconnection of the intersection point and instead the vortices rotate around each other in real time. Secondly, we showed that, when in a planar-aligning orientation, the reconnection dynamics does resemble that in 3D, with the same scaling behaviour and an irreversible transfer of incompressible energy. Finally, we discovered a qualitatively new reconnection regime

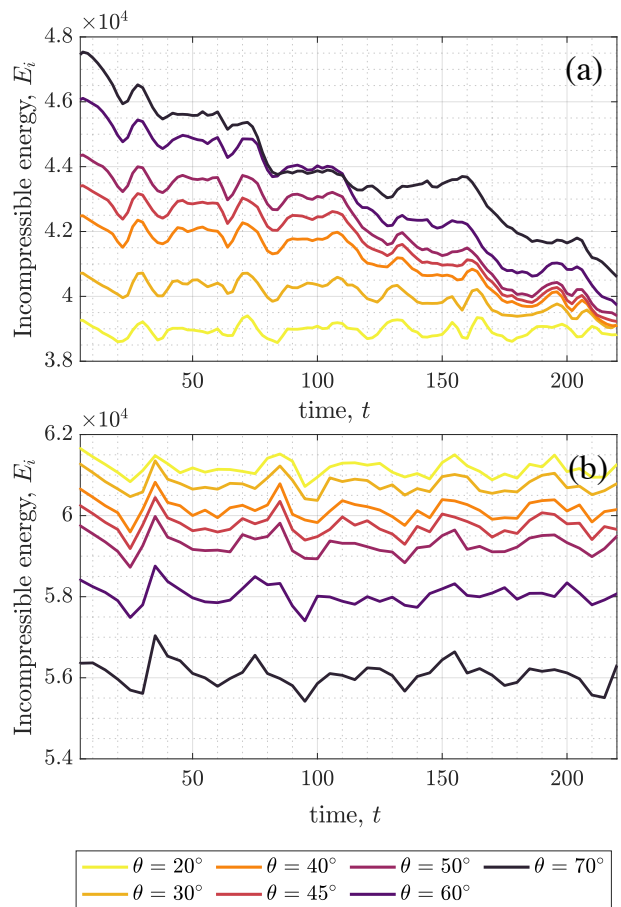


FIG. 4. The incompressible energy, E_i , over time as calculated from the numerical real-time dynamics, after the initial reconnection at $t = 0$ for different alignment angles for the (a) planar orientation and the (b) anti-aligning orientation. In the planar reconnection case, (a), we see that the incompressible energy falls for all values of θ , matching known 3D results. The anti-aligning case, however, shows a lack of loss of incompressible energy, signalling a lack of sound wave emission typically observed in 3D reconnection.

emerging in 4D when the two vortices are anti-aligned, in which the average incompressible energy does not significantly vary implying the reconnection mechanism may be time reversible. This unusual behaviour is markedly different from lower dimensions, reflecting the rich phenomenology that materialises in 4D superfluids. Going further, there are multiple interesting avenues to explore. Firstly, it would be important to explore the initiations of the instabilities in the post-reconnection state in the planar reconnection, and the characterisation of the Kelvin waves formed. Another avenue would be in understanding the consequences of a lack of loss of incompressible energy during the reconnection, and how this changes long term multi-vortex dynamics, such as turbulence. It would also be interesting to extend this study to non-orthogonal vortex pairs with

higher winding numbers k , which are expected to be dynamically-unstable towards separation into many vortex planes that could then interact in complex ways. In the very large k limit, this may lead to the formation of Abrikosov-lattice-like structures with multiple reconnection regions. In the future, it will also be interesting to identify and study closed vortex surfaces, which do not touch the system boundary, such as the analogue of 3D vortex rings and knots [17, 33, 37, 77–79], and other more exotic types of closed surfaces that may be possible in 4D [80]. Our work may also be extended to more complex 4D order parameters, motivated by the appearance of non-Abelian vortices [81, 82] in 3D spinor condensates, which exhibit richer intersection and reconnection physics. Finally, our work can be extended to more realistic experimental settings, based on techniques such as synthetic dimensions; this could involve, for example, changing the geometry of the system to make at least one of the spatial dimensions discrete or including long-range non-uniform interactions [42–66].

Acknowledgements: We thank Mike Gunn and Mark Dennis for helpful discussions. This work is supported by the Royal Society via grants UF160112, RGF\EA\180121 and RGF\R1\180071 and by the Engineering and Physical Sciences Research Council [grant number EP/W016141/1].

* h.a.j.middleton-spencer@bham.ac.uk

- [1] H. Che, J. Drake, and M. Swisdak, A current filamentation mechanism for breaking magnetic field lines during reconnection, *Nature* **474**, 184 (2011).
- [2] M. Yamada, R. Kulsrud, and H. Ji, Magnetic reconnection, *Rev. Mod. Phys.* **82**, 603 (2010).
- [3] S. Kida and M. Takaoka, Vortex reconnection, *Annu. Rev. Fluid Mech.* **26**, 169 (1994).
- [4] A. Pumir and R. M. Kerr, Numerical simulation of interacting vortex tubes, *Phys. Rev. Lett.* **58**, 1636 (1987).
- [5] D. Kleckner and W. T. Irvine, Creation and dynamics of knotted vortices, *Nat. Phys.* **9**, 253 (2013).
- [6] G. P. Bewley, M. S. Paoletti, K. R. Sreenivasan, and D. P. Lathrop, Characterization of reconnecting vortices in superfluid helium, *Proc. Natl. Acad. Sci. U.S.A.* **105**, 13707 (2008).
- [7] M. Paoletti, M. E. Fisher, and D. Lathrop, Reconnection dynamics for quantized vortices, *Physica D: Nonlinear Phenomena* **239**, 1367 (2010).
- [8] S. Serafini, L. Galantucci, E. Iseni, T. Bienaimé, R. N. Bisset, C. F. Barenghi, F. Dalfovo, G. Lamporesi, and G. Ferrari, Vortex reconnections and rebounds in trapped atomic bose-einstein condensates, *Phys. Rev. X* **7**, 021031 (2017).
- [9] E. Fonda, D. P. Meichle, N. T. Ouellette, S. Hormoz, and D. P. Lathrop, Direct observation of kelvin waves excited by quantized vortex reconnection, *Proc. Natl. Acad. Sci. U.S.A.* **111**, 4707 (2014).
- [10] S. Nazarenko and R. West, Analytical solution for nonlinear schrödinger vortex reconnection, *J. Low Temp. Phys* **132**, 1 (2003).
- [11] A. W. Baggaley, J. Laurie, and C. F. Barenghi, Vortex-density fluctuations, energy spectra, and vortical regions in superfluid turbulence, *Phys. Rev. Lett.* **109**, 205304 (2012).
- [12] L. Madeira, M. A. Caracanhas, F. dos Santos, and V. S. Bagnato, Quantum turbulence in quantum gases, *Annu. Rev. Condens. Matter Phys.* **11**, 37 (2020).
- [13] H. A. J. Middleton-Spencer, A. D. G. Orozco, L. Galantucci, M. Moreno, N. G. Parker, L. A. Machado, V. S. Bagnato, and C. F. Barenghi, Strong quantum turbulence in bose-einstein condensates, *Phys. Rev. Research* **5**, 043081 (2023).
- [14] C. F. Barenghi, H. Middleton-Spencer, L. Galantucci, and N. Parker, Types of quantum turbulence, *AVS Quantum Science* **5** (2023).
- [15] A. Villois, D. Proment, and G. Krstulovic, Evolution of a superfluid vortex filament tangle driven by the gross-pitaevskii equation, *Phys. Rev. E* **93**, 061103 (2016).
- [16] M. Leadbeater, T. Winiecki, D. Samuels, C. Barenghi, and C. Adams, Sound emission due to superfluid vortex reconnections, *Phys. Rev. Lett.* **86**, 1410 (2001).
- [17] A. Villois, D. Proment, and G. Krstulovic, Irreversible dynamics of vortex reconnections in quantum fluids, *Phys. Rev. Lett.* **125**, 164501 (2020).
- [18] K. Khani, E. Neri, L. Galantucci, F. Scazza, A. Burchianti, K.-L. Lee, C. Barenghi, A. Trombettoni, M. Inguscio, M. Zaccanti, *et al.*, Critical transport and vortex dynamics in a thin atomic josephson junction, *Phys. Rev. Lett.* **124**, 045301 (2020).
- [19] W. F. Vinen, The detection of single quanta of circulation in liquid helium ii, *Proceedings of the Royal Society of London. Series A. Mathematical and Physical Sciences* **260**, 218 (1961).
- [20] E. J. Yarmchuk, M. J. V. Gordon, and R. E. Packard, Observation of stationary vortex arrays in rotating superfluid helium, *Phys. Rev. Lett.* **43**, 214 (1979).
- [21] L. Pitaevskii, S. Stringari, and O. U. Press, *Bose-Einstein Condensation*, International Series of Monographs on Physics (Clarendon Press, 2003).
- [22] C. Pethick and H. Smith, *Bose-Einstein condensation in dilute gases* (Cambridge University Press, 2008) p. 569.
- [23] N. R. Cooper, Rapidly rotating atomic gases, *Adv. Phys.* **57**, 539 (2008).
- [24] A. L. Fetter, Rotating trapped bose-einstein condensates, *Rev. Mod. Phys.* **81**, 647 (2009).
- [25] K. W. Madison, F. Chevy, W. Wohlleben, and J. Dalibard, Vortex formation in a stirred bose-einstein condensate, *Phys. Rev. Lett.* **84**, 806 (2000).
- [26] K. W. Madison, F. Chevy, V. Bretin, and J. Dalibard, Stationary states of a rotating bose-einstein condensate: Routes to vortex nucleation, *Phys. Rev. Lett.* **86**, 4443 (2001).
- [27] M. R. Matthews, B. P. Anderson, P. C. Haljan, D. S. Hall, C. E. Wieman, and E. A. Cornell, Vortices in a bose-einstein condensate, *Phys. Rev. Lett.* **83**, 2498 (1999).
- [28] J. R. Abo-Shaeer, C. Raman, J. M. Vogels, and W. Ketterle, Observation of vortex lattices in bose-einstein condensates, *Science* **292**, 476 (2001).
- [29] N. Verhelst and J. Tempere, Vortex structures in ultracold atomic gases, *Vortex Dynamics. Intech* , 1 (2017).
- [30] K. W. Schwarz, Three-dimensional vortex dynamics in superfluid ^4He : Line-line and line-boundary interactions,

- Phys. Rev. B **31**, 5782 (1985).
- [31] J. Koplik and H. Levine, Vortex reconnection in superfluid helium, Phys. Rev. Lett. **71**, 1375 (1993).
- [32] S. Z. Alamri, A. J. Youd, and C. F. Barenghi, Reconnection of superfluid vortex bundles, Phys. Rev. Lett. **101**, 215302 (2008).
- [33] A. Vilhois, D. Proment, and G. Krstulovic, Universal and nonuniversal aspects of vortex reconnections in superfluids, Phys. Rev. Fluids **2**, 044701 (2017).
- [34] L. Galantucci, A. W. Baggaley, N. G. Parker, and C. F. Barenghi, Crossover from interaction to driven regimes in quantum vortex reconnections, Proc. Natl. Acad. Sci. U.S.A. **116**, 12204 (2019).
- [35] A. Enciso and D. Peralta-Salas, Approximation theorems for the schrödinger equation and quantum vortex reconnection, Commun. Math. Phys. **387**, 1111 (2021).
- [36] S. Zuccher, M. Caliari, A. W. Baggaley, and C. F. Barenghi, Quantum vortex reconnections, Phys. Fluids **24** (2012).
- [37] D. Proment and G. Krstulovic, Matching theory to characterize sound emission during vortex reconnection in quantum fluids, Phys. Rev. Fluids **5**, 104701 (2020).
- [38] B. V. Svistunov, Superfluid turbulence in the low-temperature limit, Phys. Rev. B **52**, 3647 (1995).
- [39] B. McCanna and H. M. Price, Superfluid vortices in four spatial dimensions, Phys. Rev. Research **3**, 023105 (2021).
- [40] B. McCanna and H. M. Price, Curved vortex surfaces in four-dimensional superfluids. i. unequal-frequency double rotations, Phys. Rev. A **110**, 013325 (2024).
- [41] B. McCanna and H. M. Price, Curved vortex surfaces in four-dimensional superfluids. ii. equal-frequency double rotations, Phys. Rev. A **110**, 013326 (2024).
- [42] O. Boada, A. Celi, J. I. Latorre, and M. Lewenstein, Quantum simulation of an extra dimension, Phys. Rev. Lett. **108**, 133001 (2012).
- [43] A. Celi, P. Massignan, J. Ruseckas, N. Goldman, I. B. Spielman, G. Juzeliūnas, and M. Lewenstein, Synthetic gauge fields in synthetic dimensions, Phys. Rev. Lett. **112**, 043001 (2014).
- [44] B. K. Stuhl, H.-I. Lu, L. M. Aycock, D. Genkina, and I. B. Spielman, Visualizing edge states with an atomic bose gas in the quantum hall regime, Science **349**, 1514 (2015).
- [45] M. Mancini, G. Pagano, G. Cappellini, L. Livi, M. Rider, J. Catani, C. Sias, P. Zoller, M. Inguscio, M. Dalmonte, and L. Fallani, Observation of chiral edge states with neutral fermions in synthetic hall ribbons, Science **349**, 1510 (2015).
- [46] B. Gadway, Atom-optics approach to studying transport phenomena, Phys. Rev. A **92**, 043606 (2015).
- [47] L. Livi, G. Cappellini, M. Diem, L. Franchi, C. Clivati, M. Frittelli, F. Levi, D. Calonico, J. Catani, M. Inguscio, and L. Fallani, Synthetic dimensions and spin-orbit coupling with an optical clock transition, Phys. Rev. Lett. **117** (2016).
- [48] T. Ozawa, H. M. Price, N. Goldman, O. Zilberberg, and I. Carusotto, Synthetic dimensions in integrated photonics: From optical isolation to four-dimensional quantum hall physics, Phys. Rev. A **93**, 043827 (2016).
- [49] L. Yuan, Y. Shi, and S. Fan, Photonic gauge potential in a system with a synthetic frequency dimension, Opt. Lett. **41**, 741 (2016).
- [50] S. Kolkowitz, S. L. Bromley, T. Bothwell, M. L. Wall, G. E. Marti, A. P. Koller, X. Zhang, A. M. Rey, and J. Ye, Spin-orbit-coupled fermions in an optical lattice clock, Nature **542**, 66 (2017).
- [51] I. Martin, G. Refael, and B. Halperin, Topological frequency conversion in strongly driven quantum systems, Phys. Rev. X **7**, 041008 (2017).
- [52] B. Sundar, B. Gadway, and K. R. Hazzard, Synthetic dimensions in ultracold polar molecules, Sci. Rep. **8**, 1 (2018).
- [53] H. M. Price, T. Ozawa, and N. Goldman, Synthetic dimensions for cold atoms from shaking a harmonic trap, Phys. Rev. A **95**, 023607 (2017).
- [54] T. Chalopin, T. Satoor, A. Evrard, V. Makhlov, J. Dalibard, R. Lopes, and S. Nascimbene, Probing chiral edge dynamics and bulk topology of a synthetic hall system, Nat. Phys. **16**, 1017 (2020).
- [55] S. K. Kanungo, J. D. Whalen, Y. Lu, M. Yuan, S. Dasgupta, F. B. Dunning, K. R. A. Hazzard, and T. C. Killian, Realizing topological edge states with rydberg-atom synthetic dimensions, Nat. Commun. **13**, 972 (2022).
- [56] E. Lustig, S. Weimann, Y. Plotnik, Y. Lumer, M. A. Bandres, A. Szameit, and M. Segev, Photonic topological insulator in synthetic dimensions, Nature **567**, 356 (2019).
- [57] A. Dutt, Q. Lin, L. Yuan, M. Minkov, M. Xiao, and S. Fan, A single photonic cavity with two independent physical synthetic dimensions, Science **367**, 59 (2020).
- [58] H. Cai, J. Liu, J. Wu, Y. He, S. Zhu, J. Zhang, and D. Wang, Experimental observation of momentum-space chiral edge currents in room-temperature atoms, Phys. Rev. Lett. **122**, 023601 (2019).
- [59] H. M. Price, T. Ozawa, and H. Schomerus, Synthetic dimensions and topological chiral currents in mesoscopic rings, Phys. Rev. Research **2**, 032017 (2020).
- [60] E. Boyers, P. J. Crowley, A. Chandran, and A. O. Sushkov, Exploring 2d synthetic quantum hall physics with a quasiperiodically driven qubit, Phys. Rev. Lett. **125**, 160505 (2020).
- [61] V. Lienhard, P. Scholl, S. Weber, D. Barredo, S. de Léséleuc, R. Bai, N. Lang, M. Fleischhauer, H. Büchler, T. Lahaye, and A. Browaeys, Realization of a density-dependent Peierls phase in a synthetic, spin-orbit coupled Rydberg system, Phys. Rev. X **10**, 021031 (2020).
- [62] C. Oliver, A. Smith, T. Easton, G. Salerno, V. Guarrera, N. Goldman, G. Barontini, and H. M. Price, Bloch oscillations along a synthetic dimension of atomic trap states, Phys. Rev. Research **5**, 033001 (2023).
- [63] C. Oliver, S. Mukherjee, M. C. Rechtstman, I. Carusotto, and H. M. Price, Artificial gauge fields in the t-z mapping for optical pulses: Spatiotemporal wave packet control and quantum hall physics, Sci. Adv. **9**, ead0360 (2023).
- [64] S. L. Cornish, M. R. Tarbutt, and K. R. Hazzard, Quantum computation and quantum simulation with ultracold molecules, Nat. Phys. **1**, 1 (2024).
- [65] M. Ehrhardt, S. Weidemann, L. J. Maczewsky, M. Heinrich, and A. Szameit, A perspective on synthetic dimensions in photonics, Laser Photonics Rev. **17**, 2200518 (2023).
- [66] T. Ozawa and H. M. Price, Topological quantum matter in synthetic dimensions, Nat. Rev. Phys. **1**, 349 (2019).
- [67] K. Viebahn, M. Sbroscia, E. Carter, J.-C. Yu, and U. Schneider, Matter-wave diffraction from a quasicrystalline optical lattice, Phys. Rev. Lett. **122**, 110404

- (2019).
- [68] J.-B. Bouhiron, A. Fabre, Q. Liu, Q. Redon, N. Mittal, T. Satoor, R. Lopes, and S. Nascimbene, Realization of an atomic quantum hall system in four dimensions, *Science* **384**, 223 (2024).
- [69] T. Ozawa and H. M. Price, Topological quantum matter in synthetic dimensions, *Nat. Rev. Phys.* , 1 (2019).
- [70] K. Hashimoto and D. Tong, Reconnection of non-abelian cosmic strings, *J. Cosmol. Astropart. Phys.* **2005** (09), 004.
- [71] A. Hanany and K. Hashimoto, Reconnection of colliding cosmic strings, *Journal of High Energy Physics* **2005**, 021 (2005).
- [72] S. Kida and M. Takaoka, Vortex reconnection, *Annu. Rev. Fluid Mech.* **26**, 169 (1994).
- [73] N. G. Berloff, Padé approximations of solitary wave solutions of the gross-pitaevskii equation, *J. Phys. A* **37**, 1617 (2004).
- [74] I. Coddington, P. Engels, V. Schweikhard, and E. A. Cornell, Observation of Tkachenko oscillations in rapidly rotating bose-einstein condensates, *Phys. Rev. Lett.* **91**, 100402 (2003).
- [75] D. P. Meikle, C. Rorai, M. E. Fisher, and D. P. Lathrop, Quantized vortex reconnection: Fixed points and initial conditions, *Phys. Rev. B* **86**, 014509 (2012).
- [76] A. J. Allen, S. Zuccher, M. Caliari, N. P. Proukakis, N. G. Parker, and C. F. Barenghi, Vortex reconnections in atomic condensates at finite temperature, *Phys. Rev. A* **90**, 013601 (2014).
- [77] D. Proment, M. Onorato, and C. F. Barenghi, Vortex knots in a bose-einstein condensate, *Phys. Rev. E* **85**, 036306 (2012).
- [78] D. Proment, M. Onorato, and C. F. Barenghi, Torus quantum vortex knots in the gross-pitaevskii model for bose-einstein condensates, *J. Phys. Conf. Ser.* **544**, 012022 (2014).
- [79] S. M. W, K. Dustin, P. Davide, K. G. L, and I. W. T. M, Helicity conservation by flow across scales in reconnecting vortex links and knots, *Proc. Natl. Acad. Sci. U.S.A.* **111**, 15350 (2014).
- [80] J. Gallier and D. Xu, *A Guide to the Classification Theorem for Compact Surfaces*, Geometry and Computing (Springer Berlin Heidelberg, 2013).
- [81] Y. Kawaguchi and M. Ueda, Spinor bose-einstein condensates, *Phys. Rep.* **520**, 253 (2012), spinor Bose-Einstein condensates.
- [82] T. Machon and G. P. Alexander, Global defect topology in nematic liquid crystals, *Proc. R. Soc. Lond.* **472**, 10.1098/rspa.2016.0265 (2016).
- [83] J. R. Munkres, *Topology*, 2nd ed. (Prentice Hall, Inc., 2000).

SUPPLEMENTARY MATERIAL

ANGULAR MOMENTUM OF SKEW INTERSECTING VORTEX PLANES

Here we will calculate the angular momentum of a generic state containing two non-orthogonal intersecting vortex planes. As in the main text, we will let one vortex span the $z^- - w^-$ plan, inducing circulation in the $x^- - y^-$ plane, while the other spans the $x^+ - y^+$, inducing circulation in the $z^+ - w^+$ plane. The transformation between the various bases is given by Eq (4) in the main text, which we will restate here in the following block matrix form

$$\mathbf{x}^\pm = \begin{pmatrix} \mathcal{C} & \mp \mathcal{S} \\ \pm \mathcal{S} & \mathcal{C} \end{pmatrix} \mathbf{x}, \quad (\text{S1})$$

where $\mathcal{C} = \text{diag}(c_1, c_2)$, and $\mathcal{S} = \text{diag}(s_1, s_2)$, and we have used the shorthand $c_j = \cos(\theta_j/2)$, $s_j = \sin(\theta_j/2)$.

We then start with the following ansatz for the order parameter describing the vortex pair

$$\psi = (x^- + iy^-) (z^+ + iw^+) g(r_1^-, r_2^+), \quad (\text{S2})$$

where r_1^- and r_2^+ are polar radii in the $x^- - y^-$ and $z^+ - w^+$ planes, respectively, and g is a real-valued and positive-definite (but otherwise unspecified) function of these radii. First we will compute the angular momenta of this state, as given by the expectation of the usual operator, $\hat{\mathbf{L}} = -i\mathbf{x} \wedge \nabla$. However, note that angular momentum cannot be transformed into a pseudovector in 4D as it can in 3D so we will need to treat it properly as an antisymmetric tensor. For our purposes, this means using the wedge product which generalises the 3D cross-product. Evaluating this operator on our ansatz using the product rule gives the following expression for the expectation value

$$\mathbf{L} = -i \int \mathbf{x} \wedge \left[\frac{\nabla(x^- + iy^-)}{x^- + iy^-} + \frac{\nabla(z^+ + iw^+)}{z^+ + iw^+} + \frac{\nabla g}{g} \right] \rho d^4x, \quad (\text{S3})$$

where we have suppressed the arguments of g for brevity. The last term is pure imaginary, and so must vanish since angular momentum is a hermitian operator. Next we will evaluate the derivatives and wedge products, using the \mathbf{x}^- coordinate frame for the first term and the \mathbf{x}^+ frame for the second, which yields

$$\mathbf{L} = \int \left[\hat{\mathbf{x}}^- \wedge \hat{\mathbf{y}}^- + \hat{\mathbf{z}}^+ \wedge \hat{\mathbf{w}}^+ - i(z^- \hat{\mathbf{z}}^- + w^- \hat{\mathbf{w}}^-) \wedge \frac{\hat{\mathbf{x}}^- + i\hat{\mathbf{y}}^-}{x^- + iy^-} - i(x^+ \hat{\mathbf{x}}^+ + y^+ \hat{\mathbf{y}}^+) \wedge \frac{\hat{\mathbf{z}}^+ + i\hat{\mathbf{w}}^+}{z^+ + iw^+} \right] \rho d^4x, \quad (\text{S4})$$

where $\hat{\mathbf{x}}^-$ denotes the unit vector in the x^- direction (and similarly for the other coordinates). The last two terms vanish by symmetry, as the integrands are odd functions of (z^-, w^-) , and (x^+, y^+) , respectively. This then gives us the following simple result without any other assumptions on the density

$$\mathbf{L} = N (\hat{\mathbf{x}}^- \wedge \hat{\mathbf{y}}^- + \hat{\mathbf{z}}^+ \wedge \hat{\mathbf{w}}^+). \quad (\text{S5})$$

Substituting in Eq (S1) we then get the following Cartesian components of \mathbf{L}

$$\mathbf{L} = N [(c_1 \hat{\mathbf{x}} + s_1 \hat{\mathbf{z}}) \wedge (c_2 \hat{\mathbf{y}} + s_2 \hat{\mathbf{w}}) + (c_1 \hat{\mathbf{z}} + s_1 \hat{\mathbf{x}}) \wedge (c_2 \hat{\mathbf{w}} + s_2 \hat{\mathbf{y}})]. \quad (\text{S6})$$

$$= N \cos \theta_- (\hat{\mathbf{x}} \wedge \hat{\mathbf{y}} + \hat{\mathbf{z}} \wedge \hat{\mathbf{w}}) + N \sin \theta_+ (\hat{\mathbf{x}} \wedge \hat{\mathbf{w}} + \hat{\mathbf{z}} \wedge \hat{\mathbf{y}}), \quad (\text{S7})$$

where $\theta_{\pm} = (\theta_1 \pm \theta_2)/2$. For anti-aligning planes, we have that $\theta_+ = 0$, and $\theta_- = \theta \in (-\pi/2, \pi/2)$, such that the total angular momentum $|\mathbf{L}|^2$ decreases as the magnitude of the tilt θ increases, as expected. For planar-aligning vortices ($\theta_+ = \theta_- = \theta$) $|\mathbf{L}|^2$ remains constant, while for aligning vortices ($\theta_+ = \theta, \theta_- = 0$) $|\mathbf{L}|^2$ increases with θ . Interestingly, aligning vortices have constant angular momenta in the original $x-y$ and $z-w$ planes, regardless of tilt. This can be explained using a special property of rotations in 4D known as isoclinic symmetry, as has been found previously [S40].

PRECESSION FREQUENCIES OF ALIGNING VORTEX PLANES

In the main text we found numerically that aligning skew vortex planes do not reconnect but instead undergo a periodic motion around each other. In this section we will try to analytically explain this motion and predict its frequency as a function of tilt angle. We will start by assuming that the motion is a rigid (double) rotation of the entire superfluid described by an angular frequency tensor $\mathbf{\Omega}$. In other words, this means that the aligning vortex planes form a stationary state in a reference frame rotating according to $\mathbf{\Omega}$. The energy $E'[\psi]$ in this rotating frame is related to that of the lab frame $E[\psi]$ by the usual formula $E'[\psi] = E[\psi] - \mathbf{\Omega} \cdot \mathbf{L}[\psi]$. Then, for any tilt angle θ , the aligning state ψ_{θ} will only be stationary if it extremises the energy E' , such that $\partial E'[\psi_{\theta}]/\partial \theta = 0$. This then gives us the following equation for the angular frequency tensor of the precession

$$\mathbf{\Omega} \cdot \frac{\partial \mathbf{L}[\psi_{\theta}]}{\partial \theta} = \frac{\partial E[\psi_{\theta}]}{\partial \theta}. \quad (\text{S8})$$

In Sec we derived the angular momentum of arbitrary skew vortex plane states [Eq (S7)], which simplifies in the aligning case to

$$\mathbf{L}[\psi_{\theta}] = N (\hat{\mathbf{x}} \wedge \hat{\mathbf{y}} + \hat{\mathbf{z}} \wedge \hat{\mathbf{w}}) + N \sin \theta (\hat{\mathbf{x}} \wedge \hat{\mathbf{w}} + \hat{\mathbf{z}} \wedge \hat{\mathbf{y}}). \quad (\text{S9})$$

The total energy in the inertial lab frame, $E[\psi]$, can be expressed hydrodynamically in terms of ρ and the velocity field from each vortex $\mathbf{v}_{1,2}$ as

$$E[\psi] = \frac{1}{2} \int (|\nabla \psi|^2 + |\psi|^4) d^4x \quad (\text{S10})$$

$$= \int \left(\frac{1}{2} \rho \mathbf{v}_1^2 + \frac{1}{2} \rho \mathbf{v}_2^2 + \rho \mathbf{v}_1 \cdot \mathbf{v}_2 + \frac{1}{2} |\nabla \sqrt{\rho}|^2 + \frac{1}{2} \rho^2 \right) d^4x. \quad (\text{S11})$$

where the first two terms are the kinetic energy of each vortex plane separately, the third is the hydrodynamic interaction between them, the fourth is the quantum pressure energy, and the last term is the interparticle interaction energy. If we evaluate this energy for an aligning state, ψ_{θ} , then the first two terms do not depend on θ due to the spherical symmetry of the system, and we will assume that the variation of last two terms with θ is negligible. This leaves us with the hydrodynamic interaction as the only term that significantly varies with theta, which for aligning states is approximated (assuming constant density ρ) by [S40]

$$E_{vv}[\psi_{\theta}] = -4\mu N \frac{\xi^2}{R^2} \ln \cos \theta \quad (\text{S12})$$

Putting these together into Eq (S8) gives the following equation for the precession frequencies

$$\Omega_{xw} + \Omega_{zy} = 4\mu \frac{\xi^2}{R^2} \frac{\tan \theta}{\cos \theta} \quad (\text{S13})$$

Assuming, by symmetry, that $\Omega_{xw} = \Omega_{zy} = \Omega$ we then get the following equation for the frequency of precession in dimensionless form

$$\Omega = \frac{2 \tan \theta}{R^2 \cos \theta}. \quad (\text{S14})$$

Note that this calculation is equivalent to an earlier result [S40] that found that skew aligning vortex plane states can form stationary states of superfluids under rotation, however the connection to vortex precession in an inertial frame was not previously made. In this previous work [S40] we found that numerically the aligning stationary states had angles and energies very close to the analytical predictions, but exhibited an avoided crossing region just like the reconnecting states we have investigated here. This raises the question of whether our assumption of rigid rotation of the aligning planes breaks down as you approach their intersection point. Further work is required to investigate this.

HODGE-HELMHOLTZ DECOMPOSITION

Given a vector field $\mathbf{F}(\mathbf{r})$ with $\mathbf{r} \in \mathbb{R}^d$, we perform the Hodge-Helmholtz decomposition

$$\mathbf{F} = -\nabla\Phi + \mathbf{R} \quad (\text{S15})$$

with ∇ the gradient operator in d dimensions, $\Phi(\mathbf{r})$ and $\mathbf{R}(\mathbf{r})$ being the scalar potential and the solenoidal (or rotational) field, respectively, by rewriting the identity in Fourier space. Expressing the Fourier transforms as

$$G_{(\cdot)}(\mathbf{k}) = \frac{1}{(2\pi)^d} \int (\cdot)(\mathbf{x}) e^{-i\mathbf{k}\cdot\mathbf{r}} d\mathbf{r} \iff (\cdot)(\mathbf{r}) = \int G_{(\cdot)}(\mathbf{k}) e^{i\mathbf{k}\cdot\mathbf{r}} d\mathbf{k} \quad (\text{S16})$$

the decomposition results in Fourier space in

$$\mathbf{G}_{\mathbf{F}} = -i\mathbf{k}G_{\Phi} + \mathbf{G}_{\mathbf{R}}. \quad (\text{S17})$$

Taking the scalar product of the last expression with $i\mathbf{k}$ and remembering that the orthogonality between the gradient of the scalar field and solenoidal field yields

$$i\mathbf{k} \cdot \mathbf{G}_{\mathbf{F}} = |\mathbf{k}|^2 G_{\Phi} \implies G_{\Phi} = i \frac{\mathbf{k} \cdot \mathbf{G}_{\mathbf{F}}}{|\mathbf{k}|^2}, \quad (\text{S18})$$

hence

$$\mathbf{G}_{\mathbf{R}} = \mathbf{G}_{\mathbf{F}} - \frac{\mathbf{k} \cdot \mathbf{G}_{\mathbf{F}}}{|\mathbf{k}|^2} \mathbf{k}. \quad (\text{S19})$$

Finally, by transforming back to physical space one obtains

$$\Phi(\mathbf{r}) = \int G_{\Phi} e^{i\mathbf{k}\cdot\mathbf{r}} d\mathbf{k} \quad (\text{S20})$$

and

$$\mathbf{R} = \int \mathbf{G}_{\mathbf{R}} e^{i\mathbf{k}\cdot\mathbf{r}} d\mathbf{k}. \quad (\text{S21})$$

DECOMPOSITION OF THE KINETIC ENERGY

The kinetic energy of a compressible fluid of density ρ and velocity \mathbf{v} is defined as

$$E_{kin} = \int \frac{1}{2} \rho |\mathbf{v}|^2 d\mathbf{r} = \int \epsilon_{kin} d\mathbf{r}, \quad (\text{S22})$$

where $\epsilon_{kin} = \frac{1}{2} \rho |\mathbf{v}|^2$ is the kinetic energy density. One defines the auxiliary vector field

$$\mathbf{f} = \frac{1}{\sqrt{2}} \sqrt{\rho} \mathbf{v} \quad (\text{S23})$$

so that, once decomposed into its orthogonal compressible (gradient of scalar potential) and incompressible (solenoidal) parts using the Hodge-Helmholtz decomposition, one has

$$\epsilon_{kin} = |\mathbf{f}|^2 = |\mathbf{f}^{(comp)}|^2 + |\mathbf{f}^{(inc)}|^2. \quad (\text{S24})$$

Therefore, the kinetic energy also follows the decomposition, namely

$$E_{kin} = E_{kin}^{(comp)} + E_{kin}^{(inc)}, \quad \text{with} \quad E_{kin}^{(comp)} = \int |\mathbf{f}^{(comp)}|^2 d\mathbf{r} \quad \text{and} \quad E_{kin}^{(inc)} = \int |\mathbf{f}^{(inc)}|^2 d\mathbf{r}. \quad (\text{S25})$$

HOMEOMORPHISM FROM RECONNECTING VORTEX PLANES TO A PUNCTURED PLANE

Here we will show that the vortex core associated with a pair of skew vortex planes after a reconnection is homeomorphic (i.e. topologically equivalent) to a single punctured plane. This change in topology from a simply connected space (a pair of intersecting lines) to a multiply connected one shows that the dynamics is truly a reconnection process in the usual sense. Firstly, two topological spaces A and B are homeomorphic if there exists a continuous bijective function between them $h : A \rightarrow B$ whose inverse $h^{-1} : B \rightarrow A$ is also continuous. This function h is called a homeomorphism between A and B . Now we will restate the linearised description of the reconnecting vortex core [Eq(5) in the main text], which is given by the following set

$$V = \{\mathbf{x} \in \mathbb{R}^4 \mid (x^- + iy^-)(z^+ + iw^+) = i\gamma\}, \quad (\text{S26})$$

where $\gamma = t(\sin \theta_2 - \sin \theta_1)$ and all relevant quantities are as defined in the main text. Technically we need to specify a topology on V before we can talk about continuity of functions. As usual for subspaces we will use the ‘‘subspace topology’’ [S83] which is the one induced by the Euclidean topology in four dimensions (the standard topology for \mathbb{R}^4). This means that a function $f : V \rightarrow A$ for any codomain A is continuous if it is the restriction of a continuous function $g : \mathbb{R}^4 \rightarrow A$ under the Euclidean topology. Next, without loss of generality, we will fix a value of $\gamma > 0$ (i.e. $\theta_1 > \theta_2$ and t fixed), which will allow us to remove γ by a rescaling of coordinates. We will also ‘‘unskew’’ the vortex core using a linear transformation. Combining both of these, we have the following linear function

$$F(\mathbf{x}) = \sqrt{\gamma} \begin{pmatrix} \mathcal{C} & \mathcal{S} \\ \mathcal{S} & \mathcal{C} \end{pmatrix}^{-1} \mathbf{x}, \quad (\text{S27})$$

where $\mathcal{C} = \text{diag}(c_1, c_2)$, and $\mathcal{S} = \text{diag}(s_1, s_2)$, and we have used the shorthand $c_j = \cos(\theta_j/2)$, $s_j = \sin(\theta_j/2)$. This function is defined provided that the given matrix inverse exists, which is true provided $\cos \theta_1 \cos \theta_2 \neq 0$. We are only considering tilt angles in the $\theta_j \in (-\pi/2, \pi/2)$, so this is automatically satisfied. Note that the excluded cases correspond to $x^- = z^+$ when $\theta_1 = \pm\pi/2$, or $y^- = w^+$ when $\theta_2 = \pm\pi/2$. In these cases the initial vortex planes intersect along a line, rather than a point, and they reconnect in the same way that vortex lines in 3D do — they form two disconnected surfaces after the reconnection. For the general case the function is an invertible linear map, and so it is a continuous bijection with a continuous inverse, i.e. a homeomorphism, from V to the space

$$F(V) = \{\mathbf{x} \in \mathbb{R}^4 \mid (x + iy)(z + iw) = i\}. \quad (\text{S28})$$

This is equivalent to a hyperbola over complex variables, which we define as $H_{\mathbb{C}} = \{(\zeta_1, \zeta_2) \in \mathbb{C}^2 \mid \zeta_1 \zeta_2 = 1\}$. To show that $H_{\mathbb{C}}$ is homeomorphic to the punctured plane given by $\mathbb{C}^{\times} = \mathbb{C} - \{0\}$, we will use a very simple homeomorphism given by projection onto either the first or second complex coordinate (i.e. either of $\zeta_{1,2}$). We will arbitrarily choose the first, such that our homeomorphism $h : H_{\mathbb{C}} \rightarrow \mathbb{C}^{\times}$ is defined as

$$h(\zeta_1, \zeta_2) = \zeta_1. \quad (\text{S29})$$

This is clearly injective (one-to-one) since $h(\zeta_1, \zeta_2) = h(\zeta'_1, \zeta'_2) \iff \zeta_1 = \zeta'_1$ from the definition of h , and therefore $\zeta_2 = 1/\zeta_1 = 1/\zeta'_1 = \zeta'_2$ from the definition of $H_{\mathbb{C}}$. It is also surjective (onto) since for any $\zeta \in \mathbb{C}^{\times}$ we have the pair $(\zeta_1, \zeta_2) = (\zeta, 1/\zeta) \in H_{\mathbb{C}}$ such that $h(\zeta_1, \zeta_2) = \zeta$. This means that h is indeed bijective, and that its inverse can be defined for all $\zeta \in \mathbb{C}^{\times}$ as

$$h^{-1}(\zeta) = (\zeta, 1/\zeta). \quad (\text{S30})$$

All that’s left is to show that both h and h^{-1} are continuous. Here we will use several well known results [S83]. Firstly, for any topological product space $A_1 \times A_2$ we can define projection functions, $p_i : A_1 \times A_2 \rightarrow A_i$ for $i \in \{1, 2\}$,

onto each factor. These take the form $p_i(a_1, a_2) = a_i$ and are both continuous functions. Secondly, any continuous function with a domain A and range B can also be considered as a continuous function from X to Y provided that X is a subset of A and that Y contains $f(X)$, the image of the restricted domain. Our function h can be defined as the projection function $p_1 : \mathbb{C}^2 \rightarrow \mathbb{C}$, with domain restricted to $H_{\mathbb{C}}$ and range restricted to $\mathbb{C}^{\times} = p_1(H_{\mathbb{C}})$ and is therefore continuous. Similarly the function $t : \mathbb{C}^{\times} \rightarrow \mathbb{C}^2$ defined as $t(\zeta) = (\zeta, 1/\zeta)$ is also continuous as both of its component functions are continuous [S83], and we can define h^{-1} by restricting the range of t to $H_{\mathbb{C}} = t(\mathbb{C}^{\times})$. Therefore h^{-1} is also continuous. This means that h is a homeomorphism between $H_{\mathbb{C}}$ and \mathbb{C}^{\times} , and so these two spaces are homeomorphic.